Geometry Distortion of the Benzene Molecule in a Strong Magnetic Field*

M. C. CAPUTO,[1] P. LAZZERETTI[2]

[1]*Departamento de Física, Facultad de Ciencias Exactas y Naturales, Universidad de Buenos Aires Ciudad Universitaria, Pab. I, Buenos Aires 1428, Argentina*
[2]*Dipartimento di Chimica dell'Università degli Studi di Modena e Reggio Emilia, Via Campi 183, Modena 41100, Italy*

ABSTRACT: The electrostatic Lorentz force acting on the H and C nuclei of a benzene molecule in the presence of a strong magnetic field with flux density **B** has been estimated via Rayleigh-Schrödinger perturbation theory to second order in **B**. In stationary conditions, a new equilibrium configuration is reached, at which the total force has been entirely transferred to the nuclei, and the force on the electrons vanishes. The distortion of the molecular geometry is rationalized in terms of third-rank electric hypershielding at the nuclei, induced by strong magnetic fields applied along three Cartesian axes. The nuclear hypershielding has been evaluated at near Hartree-Fock level of accuracy by its definition within the Rayleigh-Schrödinger perturbation theory, and by a pointwise procedure for the geometrical derivatives of magnetic susceptibilities. The connection between these two quantities is provided by the Hellmann-Feynman theorem. A field along the C_6 symmetry axis causes a symmetric contraction of the carbon ring and an elongation of the CH bonds. A field along one of the C_2 symmetry axes containing two CH bond acts to shorten them, to widen the ring, and to bend the four remaining CH bonds towards C_2. A field along one of the C_2' symmetry axes through the midpoint of two opposite CC bonds causes a spindle effect, by squeezing the molecule toward the center of mass. Constraints for rotational and translational invariance and hypervirial theorems provide a natural criterion for Hartree-Fock quality of computed nuclear electric hypershielding. However, the molecular distortion is negligible for applied fields usually available in a laboratory. © 2010 Wiley Periodicals, Inc. Int J Quantum Chem 111: 772–779, 2011

Key words: nuclear electric hypershieldings; molecular response of benzene to strong magnetic fields; distortion of molecular geometry; rotational and translational sum rules; ab initio calculations

1. Introduction

Recent advances have made available magnets providing static, spatially uniform fields of 21 T in nuclear magnetic resonance (NMR) spectroscopy [1]. Modern superconductor technology allows the use of ≈ 50 T persistent homogeneous magnets with the size needed for experimental applications [1, 2]. High-field Bitter and hybrid magnets of 100 T are expected to become accessible in the near future [3], and pulsed fields in the range of 200–2000 T are presently designed [4, 5].

The incipient availability of strong fields raises questions concerning magnitude and direction of induced changes of molecular geometry (bond lengths and angles), which may in turn affect a wide series of molecular properties. Theoretical investigations and discussion of nonlinear response of molecules in the presence of strong, persistent magnetic fields is therefore a timely issue [6–8].

A systematic study of molecular response to intense magnetic fields in the lower limit of the so-called intermediate regime, in which matter interacts with fields from 10^3 to 10^5 T [9], was undertaken in a series of previous articles [10–14], showing that cubic response produces changes of magnetizability and magnetic shielding at the nuclei, which are interpreted in terms of fourth-rank tensors, e.g., hypermagnetizabilities [15] and nuclear magnetic hypershieldings [16–18].

Magnetic field dependent magnetic properties account for a dynamic polarization of the electron distribution, which can qualitatively be explained as a feedback effect due to the Lorentz force acting on the electron current density [14, 19]. The electron charge stretches to a different equilibrium configuration to compensate for the nonlinear perturbation caused by the intense applied field. The magnetic force is entirely transferred to the nuclei, causing a variation of molecular geometry, and the average force acting upon the electrons vanishes [20].

Calculations show that the equilibrium bond length of the hydrogen molecule H_2 and of the hydrogen molecular ion H_2^+ decreases by increasing the strength of a magnetic field applied parallel to the bond direction [2]. This phenomenology can be interpreted in terms of electric field, and related Lorentz force, induced at the nuclei by the electrons of a molecule responding nonlinearly to the magnetic perturbation. The intrinsic molecular property involved is described by a third-rank tensor accounting for nuclear electric hypershielding within quadratic response in Rayleigh-Schrödinger perturbation theory (RSPT). A detailed account of the underlying theory and notation used can be found in previous articles [20–23]. Some relevant formulae are reported as Supporting Information Available (SIA).

The present study aims at investigating the quadratic response of the electrons in a benzene molecule in the presence of a strong magnetic field, via coupled Hartree-Fock (CHF) calculations of the electric hypershielding at carbon and hydrogen nuclei.

2. Results and Discussion

An extended, noncontracted (13s10p5d2f/8s4p1d) Gaussian basis set with 714 primitives [24, 25], was used to optimize molecular structural parameters at the Hartree-Fock level, $r_{CC} = 1.39503$ Å and $r_{CH} = 1.08502$ Å bond distances, with an HCH angle of 120°. The same gaugeless basis set was used to evaluate near Hartree-Fock response properties. The CHF calculation of the electric hypershielding tensors $\rho_{\alpha,\beta\gamma}^I$, for I≡C, H, was implemented within the SYSMO suite of programs [26].

The geometric derivatives of magnetizability, $\nabla_{I\alpha}\chi_{\beta\gamma}$, were calculated at the equilibrium geometry by a pointwise procedure (Properties have been calculated for five molecular geometries, i.e., at equilibrium and for nuclear displacements $\pm\delta$ along x, y, z. Magnetizability derivatives at equilibrium were obtained via numerical differentiation of an interpolation polynomial). The origin of the gauge coincides with the center of mass in all calculations. All the quantities reported in Tables I to VII are expressed in au (see Section "Magnitude of Observable Quantities" for conversion factors).

The constraints for translational and rotational invariance of geometric derivatives of magnetic susceptibility are [20–22]

$$\sum_{I=1}^{N} \nabla_{I\alpha}\chi_{\beta\gamma} = 0, \qquad (1)$$

$$\sum_{I=1}^{N} \epsilon_{\alpha\beta\gamma}R_{I\beta}\nabla_{I\gamma}\chi_{\delta\eta} = \epsilon_{\alpha\beta\delta}\chi_{\beta\eta} + \epsilon_{\alpha\beta\eta}\chi_{\delta\beta}. \qquad (2)$$

Using the Hellmann-Feynman geometric derivatives of the magnetizability tensor, see SIA, the translational and rotational sum rules are rewritten for the $\rho_{\alpha,\beta\gamma}^I$ tensor [20–22],

TABLE I

Rotational sum rule[a] for benzene hypershielding $\sum_{I=1}^{N} \epsilon_{\alpha\beta\gamma} R_{I\beta} Z_I e\rho_{\gamma,\delta\eta}^I = \epsilon_{\alpha\beta\delta}\chi_{\beta\eta} + \epsilon_{\alpha\beta\eta}\chi_{\delta\beta}$.

α	δ	η	$\epsilon_{\alpha\beta\gamma} R_{H\beta} Z_H e\rho_{\gamma,\delta\eta}^H$	$\epsilon_{\alpha\beta\gamma} R_{C\beta} Z_C e\rho_{\gamma,\delta\eta}^C$	$\sum_{I=1}^{N} \epsilon_{\alpha\beta\gamma} R_{I\beta} Z_I e\rho_{\gamma,\delta\eta}^I$	$\epsilon_{\alpha\beta\delta}\chi_{\beta\eta} + \epsilon_{\alpha\beta\eta}\chi_{\delta\beta}$
x	y	y	0.272E−04	−0.108E−03	−0.806E−04	0.564E−05
x	y	z	−0.115E−03	−0.513E−04	−0.167E−03	−0.109E−03
x	z	z	−0.307E−04	0.651E−04	0.344E−04	−0.564E−05
y	x	y	−0.929E−05	0.777E−06	−0.851E−05	−0.282E−05
y	x	z	0.432E+01	0.104E+02	0.147E+02	0.145E+02
z	x	y	−0.432E+01	−0.104E+02	−0.147E+02	−0.145E+02
z	z	x	−0.446E−05	0.548E−05	0.101E−05	0.282E−05

[a] In SI atomic units. Coordinates of nuclei, in bohr. C_1: (0., 0., 2.63622); H_1: (0., 0., 4.68661); C_2: (0., 2.28303, 1.31811); H_2: (0., 4.05872, 2.34331).

$$\sum_{I=1}^{N} Z_I e\rho_{\alpha,\beta\gamma}^I = 0, \qquad (3)$$

$$\sum_{I=1}^{N} \epsilon_{\alpha\beta\gamma} R_{I\beta} Z_I e\rho_{\gamma,\delta\eta}^I = \epsilon_{\alpha\beta\delta}\chi_{\beta\eta} + \epsilon_{\alpha\beta\eta}\chi_{\delta\beta}. \qquad (4)$$

The translational sum rules, Eqs. (1) and (3), are satisfied by symmetry in the present case of benzene, and they cannot be used to test the quality of the calculation. At any rate, within the purpose of the present study, calculated magnetizabilities are virtually the same as those obtained via the same basis basis set allowing for the procedure of continuous transformation of the origin of the current density [24, 25], and can accordingly be considered virtually invariant to a gauge translation. Near Hartree-Fock quality can therefore be expected also for geometrical derivative.

However, the theoretical results for the rotational sum rule, presented in Table I, give clear indications on the accuracy of computed hypershieldings reported in Tables II, IV, VI, and VII. In fact, the calculated nonvanishing left- and right-hand sides of Eq. (4) are coincident to three significant figures in most cases.

The electric hypershieldings obtained analytically by the defining relationships, see SIA, are compared, in Tables III and V, with the corresponding geometrical derivatives of magnetizability determined via a pointwise procedure. The overall agreement for all the components is excellent, discrepancies being generally quite small. The conditions of permutational and point-group symmetry, e.g., $\rho_{x,yz}^I = \rho_{x,zy}^I = \rho_{y,xy}^I = \rho_{y,yx}^I$, $\rho_{z,xy}^I = -\rho_{y,zx}^I$ for $I\equiv C_1$ and $I\equiv H_1$, are satisfied.

In conclusion, the nuclear hypershieldings evaluated in this study, and reported in Tables II, IV, VI, and VII, are judged to be of near Hartree-Fock quality.

Inspection of the Tables, and of Figures 1–3, shows the effect of a strong magnetic field on the molecular geometry. For $B_x \parallel C_6$, the $\rho_{z,xx}^C$ component is negative, whereas $\rho_{z,xx}^H$ is positive, indicating a symmetrical displacement of the C nuclei toward the center of

TABLE II

Diamagnetic and paramagnetic contributions to the electric hypershielding at the carbon nucleus of benzene.[a]

$\alpha\beta\gamma$	$\rho_{\alpha\beta\gamma}^{dC_1}$	$\rho_{\alpha\beta\gamma}^{pC_1}$	$\rho_{\alpha\beta\gamma}^{C_1}$
xzx	0.690	−0.472	0.218
yzy	0.677	−0.759	−0.082
zxx	−1.273	0.894	−0.379
zyy	−1.236	1.088	−0.148
zzz	−0.104	0.399	0.295

[a] In SI atomic units. Coordinates of carbon nucleus, in bohr: $C_1 \equiv (0., 0., 2.63622)$.

TABLE III

Comparison between numerical derivatives and analytical electric hypershielding at the carbon nucleus of benzene.[a]

$\alpha\beta\gamma$	$\nabla_\alpha \chi_{\beta\gamma}^d/Z_C$	$\rho_{\alpha\beta\gamma}^{dC_1}$	$\nabla_\alpha \chi_{\beta\gamma}^p/Z_C$	$\rho_{\alpha\beta\gamma}^{pC_1}$	$\nabla_\alpha \chi_{\beta\gamma}^{tot}/Z_C$	$\rho_{\alpha\beta\gamma}^{C_1}$
zxx	−1.272	−1.273	0.896	0.894	−0.376	−0.379
zyy	−1.236	−1.236	1.095	1.088	−0.141	−0.148
zzz	−0.104	−0.104	0.400	0.399	0.296	0.295

[a] In SI atomic units. Coordinates of carbon nucleus, in bohr: $C_1 \equiv (0., 0., 2.63622)$; H_1: (0., 0., 4.68661).

TABLE IV

Diamagnetic and paramagnetic contributions to the electric hypershielding at the hydrogen nucleus of benzene.[a]

$\alpha\beta\gamma$	$\rho_{\alpha\beta\gamma}^{dH_1}$	$\rho_{\alpha\beta\gamma}^{pH_1}$	$\rho_{\alpha\beta\gamma}^{H_1}$
xzx	0.943	−0.636	0.307
yzy	0.957	−0.383	0.574
zxx	−2.458	2.988	0.530
zyy	−2.555	2.029	−0.526
zzz	−0.113	−0.168	−0.281

[a] In SI atomic units. Coordinates of the hydrogen nucleus, in bohr: $H_1 \equiv (0., 0., 4.68661)$.

mass and an elongation of the CH bonds. Therefore, a strong magnetic field at right angles to the plane of the nuclei of a benzene molecule causes a global contraction of the carbon ring and an expansion of the regular hexagon with the hydrogen nuclei at its vertices, as shown in Figure 1.

A strong magnetic field $B_z \parallel C_2$ causes expansion of the carbon ring and shortening of the CH bond in the z the direction, as the $\rho_{z,zz}^C$ and $\rho_{z,zz}^H$ components have opposite sign. The two pairs of CH bonds on either side of the C_2 symmetry axes tend to contract and tilt toward the direction of B_z, as one can see in Figure 2.

Strong uniform static magnetic fields compress the electronic distribution, and exert a centripetal force, depending on the second power of **B**, see the SIA, which pushes charge inward via a spindle effect in atoms and in diatropic systems like benzene, sustaining diamagnetic ring currents (linear in **B**) about the external magnetic field. For B_y parallel to the C_2' symmetry axis, this effect [11, 13, 14], squeezing and elongating the molecular skeleton about the direction of the magnetic field, is observed in Figure 3,

TABLE V

Comparison between numerical derivatives and analytical electric hypershielding at the hydrogen nucleus of benzene.[a]

$\alpha\beta\gamma$	$\nabla_\alpha \chi_{\beta\gamma}^{d}$	$\rho_{\alpha\beta\gamma}^{dH_1}$	$\nabla_\alpha \chi_{\beta\gamma}^{p}$	$\rho_{\alpha\beta\gamma}^{pH_1}$	$\nabla_\alpha \chi_{\beta\gamma}^{tot}$	$\rho_{\alpha\beta\gamma}^{H_1}$
zxx	−2.461	−2.458	2.979	2.987	0.518	0.529
zyy	−2.558	−2.555	2.018	2.029	−0.540	−0.526
zzz	−0.113	−0.113	−0.166	−0.168	−0.278	−0.281

[a] In SI atomic units. Coordinates of the hydrogen nucleus, in bohr: $H_1 \equiv (0., 0., 4.68661)$.

TABLE VI

Diamagnetic and paramagnetic contributions to the electric hypershielding at the carbon nucleus of benzene.[a]

$\alpha\beta\gamma$	$\rho_{\alpha\beta\gamma}^{dC_2}$	$\rho_{\alpha\beta\gamma}^{pC_2}$	$\rho_{\alpha\beta\gamma}^{C_2}$
xyx	0.598	−0.409	0.189
xzx	0.345	−0.236	0.109
yxx	−1.102	0.774	−0.328
yyy	−0.042	0.166	0.124
yzy	0.255	−0.069	0.187
yzz	−1.119	1.122	0.003
zxx	−0.636	0.447	−0.189
zyy	−0.701	0.855	0.154
zzy	0.538	−0.478	0.061
zzz	0.031	−0.111	0.080

[a] In SI atomic units. Coordinates of the carbon nucleus, in bohr: $C_2 \equiv (0., 2.28303, 1.31811)$.

consistent with the sign of the $\rho_{y,yy}^C$, $\rho_{z,yy}^C$, $\rho_{y,yy}^H$, and $\rho_{z,yy}^H$ components.

3. Magnitude of Observable Quantities

An external magnetic field **B** induces an electric field

$$\Delta\langle \hat{E}_{I\alpha}^n \rangle = \frac{1}{2} \rho_{\alpha,\beta\gamma}^I B_\beta B_\gamma \tag{5}$$

TABLE VII

Diamagnetic and paramagnetic contributions to the electric hypershielding at the hydrogen nucleus of benzene.[a]

$\alpha\beta\gamma$	$\rho_{\alpha\beta\gamma}^{dH_2}$	$\rho_{\alpha\beta\gamma}^{pH_2}$	$\rho_{\alpha\beta\gamma}^{H_2}$
xyx	0.817	−0.551	0.266
xzx	0.472	−0.318	0.154
yxx	−2.129	2.587	0.458
yyy	0.212	0.164	−0.048
yzy	0.677	−0.728	−0.051
yzz	−2.099	1.447	−0.651
zxx	−1.229	1.494	0.265
zyy	−1.080	0.478	−0.602
zzy	0.943	−0.641	0.302
zzz	−0.255	0.452	0.198

[a] In SI atomic units. Coordinates of the hydrogen nucleus, in bohr: $H_2 \equiv (0., 4.05872, 2.34331)$.
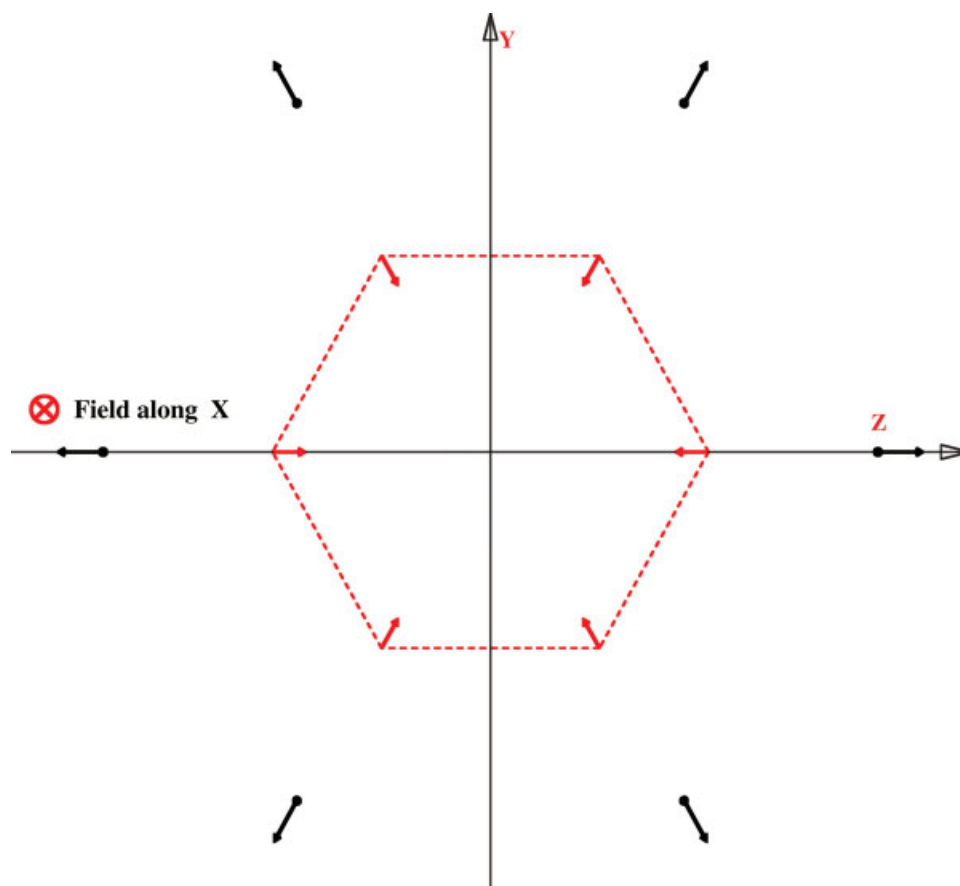
FIGURE 1. Geometrical distortion of the benzene molecule in a field applied along the $C_6 \equiv x$ axis. Red (black) arrows indicate the direction of C (H) nuclear displacements. [Color figure can be viewed in the online issue, which is available at wileyonlinelibrary.com.]

at nucleus I in a molecule by the quadratic response of n electrons [20–23]. Such a field exerts a Lorentz force $\Delta\langle\hat{F}_I^n\rangle = Z_I e \Delta\langle\hat{E}_I^n\rangle$ on nucleus I and causes a distortion of geometry of a molecule toward a new equilibrium configuration. The electric hypershielding has dimension $V\,m^{-1}T^{-2} \equiv kg^{-1}\,m\,s\,A$ in the SI system of units. The calculations were carried out using the following base units: [27] mass $m_e = 9.10938188 \times 10^{-31}$ kg, charge $e = 1.602176462 \times 10^{-19}$ C, action $\hbar = 1.054571596 \times 10^{-34}$ J s, permittivity $\kappa_0 = 4\pi\epsilon_0$, $\epsilon_0 = 8.854187817\ldots \times 10^{-12}\,F\,m^{-1}$. Derived units are e.g., the bohr $a_0 = 0.5291772083 \times 10^{-10}$ m, the hartree $E_h = m_e e^4/\kappa_0^2\hbar^2 = e^2/\kappa_0 a_0 = 4.35974381 \times 10^{-18}$ J, etc. The CODATA recommended values for the base and derived units are taken from Mohr and Taylor [28].

For the analytic electric hypershielding $\rho_{\alpha,\beta\gamma}^I$, and the numerical geometrical derivative of the magnetizability $1/(Z_I e)\nabla_{I\alpha}\chi_{\beta\gamma}$, given in au in the

Tables I–VII, the conversion factor from au to SI units is $9.30727549\,V\,m^{-1}\,T^{-2}$. For $\chi_{\alpha\beta}$, the conversion factor from au to SI units per molecule is $7.89103641 \times 10^{-29}\,J\,T^{-2}$.

Absolute values of $\rho_{\alpha,\beta\gamma}^I$ calculated in the present article vary in the range $\approx$0.3–0.6 au, for the hydrogen nucleus, and $\approx$0.1–0.4 au for the carbon nucleus. The corresponding electric fields at the nuclei are, for B expressed in tesla, $\Delta\langle\hat{E}_H^n\rangle \approx 1.4B^2$–$2.8B^2\,V\,m^{-1}$ for H, and $\Delta\langle\hat{E}_C^n\rangle \approx 0.5B^2$–$1.9B^2\,V\,m^{-1}$ for C. The force $\Delta\langle\hat{F}_H^n\rangle = Z_H e\Delta\langle\hat{E}_H^n\rangle$ acting on the hydrogen nucleus is $\approx$2.2 $\times 10^{-19}B^2$–$4.4 \times 10^{-19}B^2$ N, that acting on the carbon nucleus is $\Delta\langle\hat{F}_C^n\rangle = Z_C e\Delta\langle\hat{E}_C^n\rangle \approx 4.8 \times 10^{-19}B^2$–$1.1 \times 10^{-18}B^2$ N.

A rough estimate of C–H and C–C bond length changes caused by the strong applied field can be obtained from the harmonic force constant for the C–H and C–C bond stretching determined by vibrational spectroscopy and/or predicted by ab initio
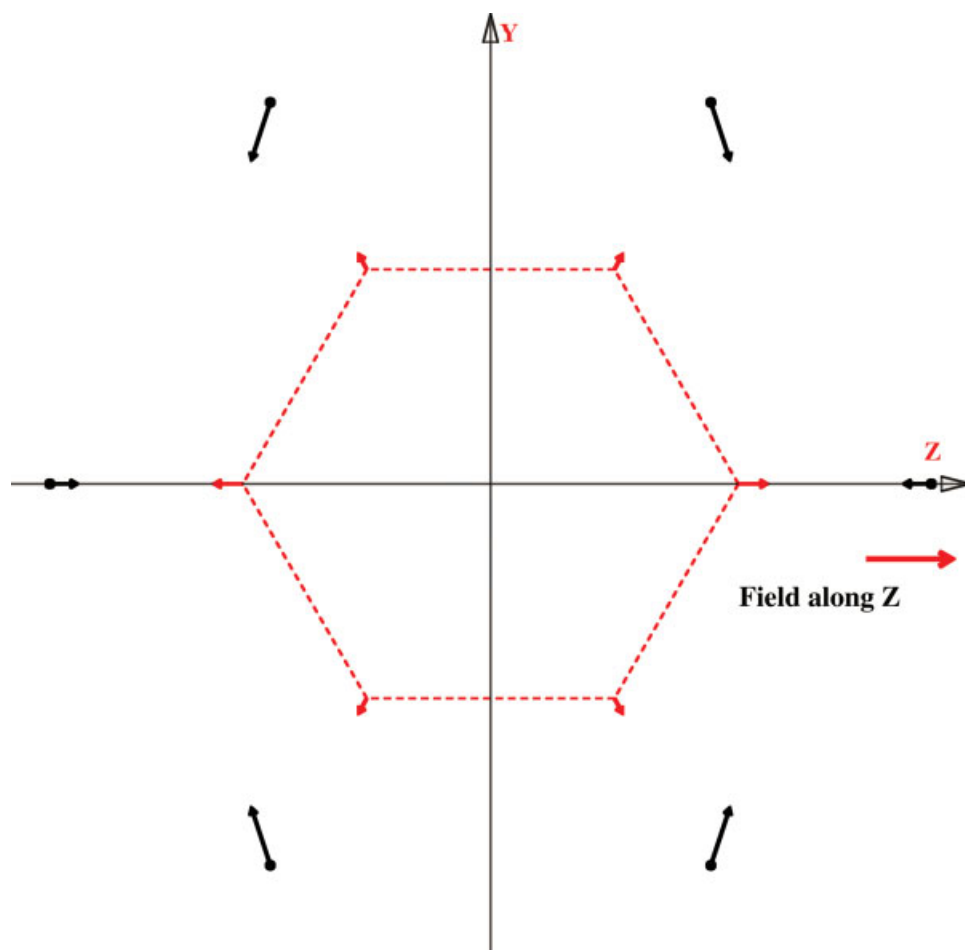
FIGURE 2. Geometrical distortion of the benzene molecule in a field applied along the $C_2 \equiv z$ axis. [Color figure can be viewed in the online issue, which is available at wileyonlinelibrary.com.]

and density-functional calculations [29–31]. With $k_{CH} = 5.547 \times 10^2 \, \mathrm{N\,m^{-1}}$, and $k_{CC} = 6.616 \times 10^2 \, \mathrm{N\,m^{-1}}$ [29], the displacement of H and C nuclei due to the strong external magnetic field produces a change $\delta r = \langle \hat{F}_z^n \rangle / k_{CH} = (1/2)(Z_C \rho_{z,zz}^C + Z_H \rho_{z,zz}^H) B^2 / k_{CH} \approx 2.00 \times 10^{-21} B^2 \, \mathrm{m}$ of the C–H bond distance. The change of C–C bond length is analogously estimated by $\delta r = \langle \hat{F}_z^n \rangle / k_{CC} = Z_C \rho_{z,zz}^C B^2 / k_{CC} \approx 3.99 \times 10^{-21} B^2 \, \mathrm{m}$.

As the equilibrium bond distances for the benzene molecule in the absence of field, are $r_{CH} = 1.077 \times 10^{-10} \, \mathrm{m}$ and $r_{CC} = 1.395 \times 10^{-10} \, \mathrm{m}$ [30], δr values of such a magnitude are negligible unless $B = |\mathbf{B}|$ approaches $1 \, \mathrm{au} = \hbar/ea_0 = 2.350517349 \times 10^5 \, \mathrm{T}$.

The equation $Z_I e \rho_{\alpha,\beta\gamma}^I = \nabla_{I\alpha} \chi_{\beta\gamma}$ can be used to estimate the change of magnetizability caused by molecular vibration. Allowing for the hypershielding values in Table IV and the numerical derivatives in Table V, a 0.1 Bohr displacement of one hydrogen nucleus decreases the in-plane component of the magnetic susceptibility, $\chi_\perp \equiv \chi_{yy} = \chi_{zz}$, by ≈ -0.03 SI au, and increases the out-of-plane $\chi_\parallel \equiv \chi_{xx}$ by ≈ 0.05 SI au. Therefore this change of C–H bond length would affect the experimental values [32] $\chi_\perp = -7.34$ and $\chi_\parallel = -19.91$ SI au to the second decimal place.

4. Conclusions

The electric shielding tensors at the carbon ad hydrogen nuclei of the benzene molecule in an external magnetic field have been evaluated at the Hartree-Fock level. The accuracy of the calculation has been assessed via sum rules for translational and rotational invariance, and by comparison of analytic and numerical geometrical derivatives. The
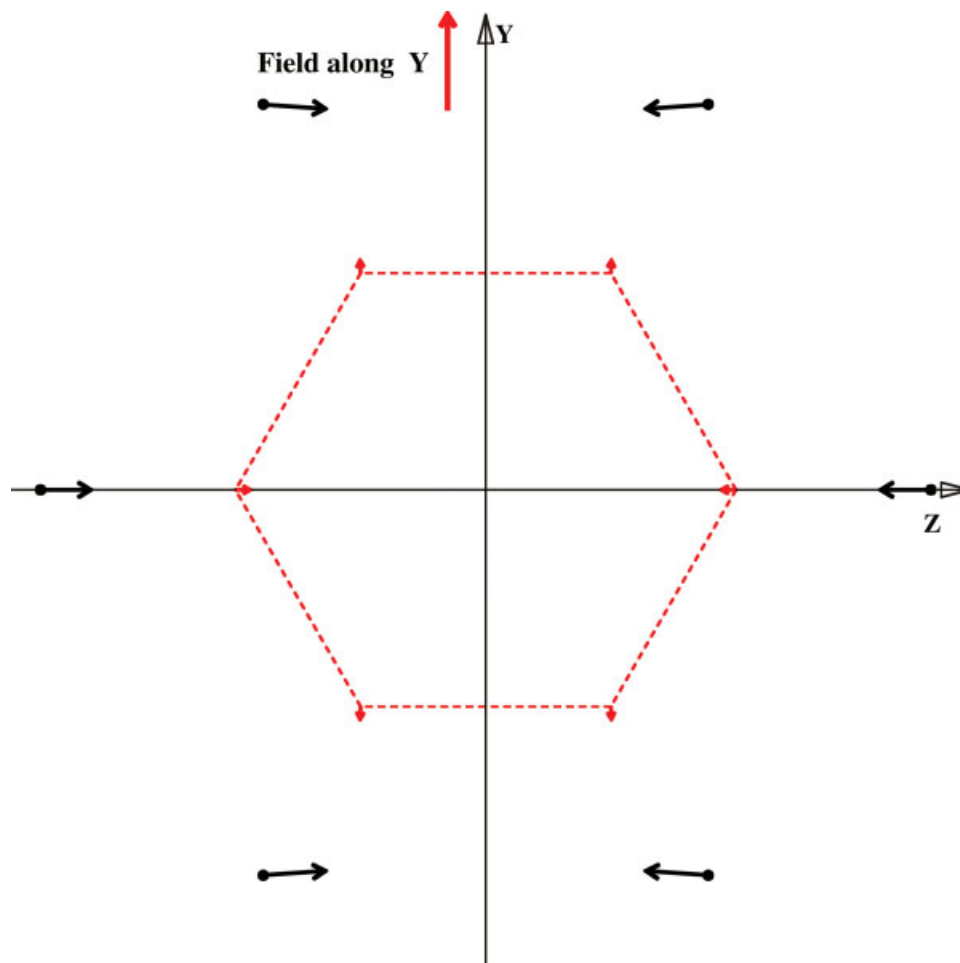
FIGURE 3. Geometrical distortion of the benzene molecule in a field applied along the $C_2' \equiv y$ axis. [Color figure can be viewed in the online issue, which is available at wileyonlinelibrary.com.]

calculations show that molecular distortion caused by quadratic response to magnetic fields presently available in a laboratory is too small to be observed with current magnetic fields.

References

1. van Bentum, P. J. M.; Maan, J. C.; van Os, J.; Kentgens, A. P. M. Chem Phys Lett 2003, 376, 338.

2. Runge, K.; Sabin, J. R. Int J Quantum Chem 1997, 64, 561.

3. Schmelcher, P.; Cederbaum, L. S. Int J Quantum Chem 1997, 64, 501.

4. Jost, R. Int J Quantum Chem 1997, 64, 571.

5. Solem, J. C.; Sheppard, M. G. Int J Quantum Chem 1997, 64, 619.

6. Zaric, S.; Ostojic, G. N.; Kono, J.; Shaver, J.; Moore, V. C.; Strano, M. S.; Hauge, R. H.; Smalley, R. E.; Wei, X. Science 2004, 304, 1129.

7. Coskun, U. C.; Wei, T.-C.; Vishveshwara, S.; Goldbart, P. M.; Bezryadin, A. Science 2004, 304, 1132.

8. Compernolle, S.; Chibotaru, L. F.; Ceulemans, A. Chem Phys Lett 2006, 428, 119.

9. Lai, D. Rev Mod Phys 2001, 73, 629.

10. Pagola, G. I.; Caputo, M. C.; Ferraro, M. B.; Lazzeretti, P. J Chem Phys 2004, 120, 9556.

11. Pagola, G. I.; Caputo, M. C.; Ferraro, M. B.; Lazzeretti, P. Chem Phys Lett 2004, 400, 133.

12. Pagola, G. I.; Caputo, M. C.; Ferraro, M. B.; Lazzeretti, P. Chem Phys Lett 2005, 408, 403.

13. Pagola, G. I.; Caputo, M. C.; Ferraro, M. B.; Lazzeretti, P. J Chem Phys 2005, 122, 074318.1/6.

14. Pagola, G. I.; Caputo, M. C.; Ferraro, M. B.; Lazzeretti, P. Phys Rev A 2005, 72, 033401:1–8.

15. Žaucer, M.; Ažman, A. Phys Rev A 1977, 16, 475.

16. Ramsey, N. F. Phys Rev A 1970, 1, 1320.

17. Vaara, J.; Manninen, P.; Lounila, J. Chem Phys Lett 2003, 372, 750.

18. Manninen, P.; Vaara, J. Phys Rev A 2004, 69, 022503.

2

19. Soncini, A.; Fowler, P. W. Chem Phys Lett 2004, 400, 213.

20. Lazzeretti, P.; Defranceschi, M.; Berthier, G. Adv Quantum Chem 1995, 26, 1.

21. Lazzeretti, P. In Handbook of Molecular Physics and Quantum Chemistry; Wilson, S., Ed.; John Wiley & Sons, Ltd.: Chichester, 2003; Vol. 3, Part 1, Chapter 3, p 53.

22. Lazzeretti, P. Theor Chem Acc 2006, 116, 420.

23. Caputo, M. C.; Ferraro, M. B.; Pagola, G. I.; Lazzeretti, P. J Chem Phys 2007, 126, 154103-1/9.

24. Ferraro, M. B.; Faglioni, F.; Ligabue, A.; Pelloni, S.; Lazzeretti, P. Magn Res Chem 2005, 43, 316.

25. Zanasi, R.; Lazzeretti, P.; Malagoli, M.; Piccinini, F. J Chem Phys 1995, 102, 7150.

26. Lazzeretti, P.; Malagoli, M.; Zanasi, R. Technical Report on Project "Sistemi Informatici e Calcolo Parallelo", Research Report 1/67, CNR, 1991.

27. McWeeny, R. Nature 1973, 243, 196.

28. Mohr, P. J.; Taylor, B. N. Rev Mod Phys 2000, 72, 351; Table XXVIII.

29. Rashev, S.; Moule, D. C. J Phys Chem A 2004, 108, 1259.

30. Bérces, A.; Ziegler, T. J Chem Phys 1993, 98, 4793.

31. Martin, J. M. L.; Taylor, P. R.; Lee, T. J. Chem Phys Lett 1997, 275, 414.

32. Hoarau, J.; Lumbroso, N.; Pacault, A. Compt Rend Hebd Acad Sci (Paris) 1956, 242, 1702.